

# Development of a gene edited next-generation hematopoietic cell transplant to enable acute myeloid leukemia treatment by solving off-tumor toxicity

John R. Lydeard,<sup>1</sup> Michelle I. Lin,<sup>1</sup> Huanying Gary Ge,<sup>1</sup> Amanda Halfond,<sup>1</sup> Shu Wang,<sup>1</sup> Mark B. Jones,<sup>1</sup> Julia Etchin,<sup>1</sup> Gabriella Angelini,<sup>1</sup> Juliana Xavier-Ferruccio,<sup>1</sup> Jessica Lisle,<sup>1</sup> Kienan Salvatore,<sup>1</sup> Yonina Keschner,<sup>1</sup> Hannah Mager,<sup>1</sup> Julian Scherer,<sup>1</sup> Jianxin Hu,<sup>1</sup> Siddhartha Mukherjee,<sup>2,3,4</sup> and Tirtha Chakraborty<sup>1,4</sup>

<sup>1</sup>Vor Biopharma, Cambridge, MA 02140, USA; <sup>2</sup>Department of Medicine, Columbia University Irving Cancer Research Center, Columbia University, New York, NY 10032, USA; <sup>3</sup>Edward P. Evans Center for Myelodysplastic Syndromes at Columbia University, New York, NY 10032, USA

**Immunotherapy of acute myeloid leukemia (AML) has been challenging because the lack of tumor-specific antigens results in “on-target, off-tumor” toxicity. To unlock the full potential of AML therapies, we used CRISPR-Cas9 to genetically ablate the myeloid protein CD33 from healthy donor hematopoietic stem and progenitor cells (HSPCs), creating tremtelectogene empogeditemcel (trem-cel). Trem-cel is a HSPC transplant product designed to provide a reconstituted hematopoietic compartment that is resistant to anti-CD33 drug cytotoxicity. Here, we describe preclinical studies and process development of clinical-scale manufacturing of trem-cel. Preclinical data showed proof-of-concept with loss of CD33 surface protein and no impact on myeloid cell differentiation or function. At clinical scale, trem-cel could be manufactured reproducibly, routinely achieving >70% CD33 editing with no effect on cell viability, differentiation, and function. Trem-cel pharmacology studies using mouse xenograft models showed long-term engraftment, multilineage differentiation, and persistence of gene editing. Toxicology assessment revealed no adverse findings, and no significant or reproducible off-target editing events. Importantly, CD33-knockout myeloid cells were resistant to the CD33-targeted agent gemtuzumab ozogamicin *in vitro* and *in vivo*. These studies supported the initiation of the first-in-human, multicenter clinical trial evaluating the safety and efficacy of trem-cel in patients with AML (NCT04849910).**

## INTRODUCTION

Acute myeloid leukemia (AML) is the most common leukemia in adults, with a 5-year survival rate of <30%.<sup>1,2</sup> For decades, allogeneic hematopoietic cell transplantation (HCT) has been the standard of care for patients at high risk of relapse; >3,300 allogeneic HCTs for AML were performed in 2020 in the United States.<sup>3</sup> Yet, relapse-free and overall survival for many patients remains poor.<sup>4,5</sup>

Antigen-specific immunotherapies, including antibody drug conjugates and chimeric antigen receptor (CAR)-T cells, are emerging ap-

proaches for treating cancer. These require cell surface makers that are exclusively or preferentially expressed on cancer cells to minimize toxicity against healthy cells, or “on-target, off-tumor” toxicity. However, AML antigens, such as the transmembrane receptor CD33, are also expressed on the surface of normal myeloid cells and/or myeloid progenitors,<sup>6</sup> thus limiting the application of antigen-directed therapies. CD33-directed therapies, including anti-CD33 CAR-T cells and the Food and Drug Administration-approved agent gemtuzumab ozogamicin (GO, Mylotarg), have shown significant anti-leukemic activity in both preclinical and clinical studies of AML but are hampered by severe myelotoxicity due to on-target, off-tumor activity.<sup>7–10</sup>

While the exact function of CD33 is poorly defined, evidence suggests a role in modulating the immune response in humans.<sup>11</sup> The identification of humans with homozygous loss-of-function (LOF) CD33 mutations provides compelling evidence that CD33 is dispensable.<sup>12–15</sup> The Genome Aggregation Database currently includes 65 individuals reported to be homozygous for CD33 LOF mutations while analysis of the UK Biobank database identified at least 176 individuals with homozygous LOF mutations in CD33.<sup>12,13</sup> Analysis of healthy phenotypes and age distributions of those with LOF mutations suggest there is no effect on fitness and health (supplemental material).<sup>12,14–16</sup> Since multiple receptors within the CD33-related Siglec family are expressed on hematopoietic cells,<sup>17,18</sup> the absence of phenotype may be due to functional redundancy or compensation by other family members. Moreover, it has been demonstrated that CD33 can be experimentally ablated from human HSPCs without any discernible impairment of hematopoietic or immunological function. The resulting CD33 null hematopoietic cells also display resistance to CD33-targeted therapies.<sup>15,19,20</sup>

Received 23 June 2023; accepted 11 October 2023;  
<https://doi.org/10.1016/j.omtm.2023.101135>.

<sup>4</sup>These authors contributed equally

**Correspondence:** John R. Lydeard, Vor Biopharma, Cambridge, MA 02140, USA.  
**E-mail:** [jlydeard@vorbio.com](mailto:jlydeard@vorbio.com)



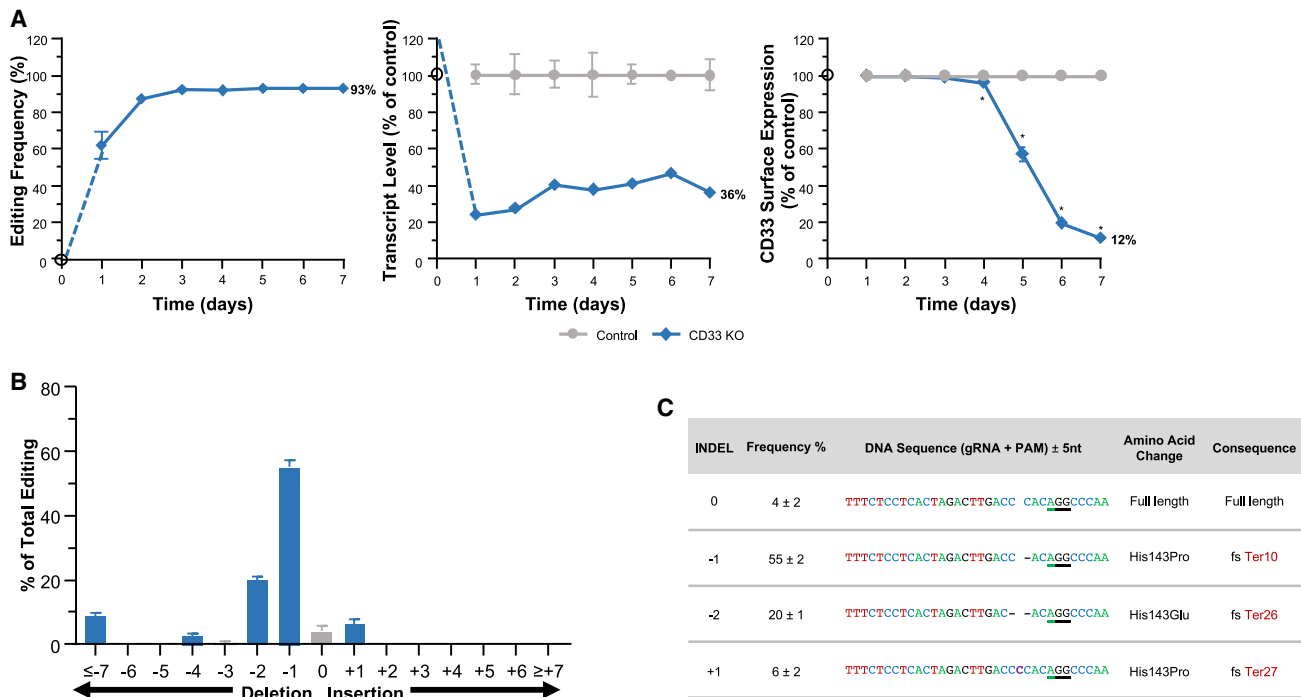


**Figure 1. Molecular consequence of CD33-KO**

(A) HL-60 cells were electroporated with the Cas9-RNP (CD33-KO) or without the Cas9-RNP (control);  $n = 3$  per condition. Editing frequency was assessed by ICE analysis, transcript expression by ddPCR (CD33 normalized to glucuronidase beta and percentage of averaged control), and CD33 cell surface protein expression by flow cytometry (percentage of control). Data are represented as mean  $\pm$  SD. Comparisons were performed using Student's *t* test; \* $p < 0.05$ . (B) Frequency of the most common indels in HL-60 CD33-KO cells 7 days post-electroporation, as a percentage of total editing events. Data are represented as mean  $\pm$  SD,  $n = 3$ . (C) DNA sequence of the CD33 target region, gRNA+PAM  $\pm 5$  nucleotides. Dash represents deletion, "C" represents the identified nucleotide insertion. Each indel results in an amino acid substitution at position 143 of the coding sequence, leading to a downstream frameshift (fs) and subsequent termination (Ter). The number following "Ter" represents the number of amino acids following the insertion.

We have developed an approach to eliminate on-target toxicity of CD33-directed therapies by genetically ablating CD33 from healthy donor HSPCs using CRISPR-Cas9 (Figure S1). The CD33-null HSPC drug product is referred to as tremtelectogene empogeditemcel (trem-cel; formerly VOR33). Trem-cel is an allogeneic, human leukocyte antigen-matched, genome-edited product intended for administration to HCT-eligible patients with AML who are at high risk for leukemia relapse and post-transplant mortality. The reconstituted hematopoietic compartment of patients receiving trem-cel is expected to be resistant to cytotoxicity induced by CD33-targeted agents such as GO and therefore allow delivery of these therapeutics with minimal toxicity against the transplanted hematopoietic cells. This approach has the potential to enable CD33-directed therapies by allowing administration at optimal doses and schedules without dose delays or omissions. Here we describe the preclinical assessment and scale-up process for trem-cel, in preparation for clinical manufacturing, which supported the ongoing first-in-human clinical trial of trem-cel in patients with AML.

## RESULTS

### Gene editing resulted in loss of CD33

In HL-60 CD33-knockout (KO) cells, we observed >90% editing by day 3 post-electroporation and near-complete loss of CD33 surface

protein at day 7 after electroporation (Figure 1A). As this was a single guide RNA (gRNA)-mediated edit, we wanted to ensure that the CD33 transcript was promptly degraded otherwise it could lead to generation of aberrant and potentially undetectable polypeptides. As editing plateaus 3 days post-electroporation, CD33 transcript decreased to  $\sim 35\%$  of control (Figure 1A). Repair of the Cas9-induced DNA double-strand break by the non-homologous end-joining (NHEJ) repair pathway can lead to nucleotide indels that can disrupt the open reading frame and result in loss of the full-length protein. The most common indels observed were 1-base pair (bp) deletions, 2-bp deletions, and 1-bp insertions (Figure 1B), all of which resulted in a frameshift and premature termination in the immunoglobulin-like constant-2-type domain encoded by exon 3 (Figure 1C).

### CD33 deletion did not affect distribution of HSPC subpopulations

Next, we assessed the impact of CD33 protein loss on primary human HSPCs generated at research scale. Human CD34+ HSPCs represent a heterogeneous cell population that consists of both stem and multiple progenitor subpopulations, including long-term hematopoietic stem cells (LT-HSCs).<sup>21-23</sup> Two of the defining features of LT-HSCs are their ability to maintain long-term engraftment and support

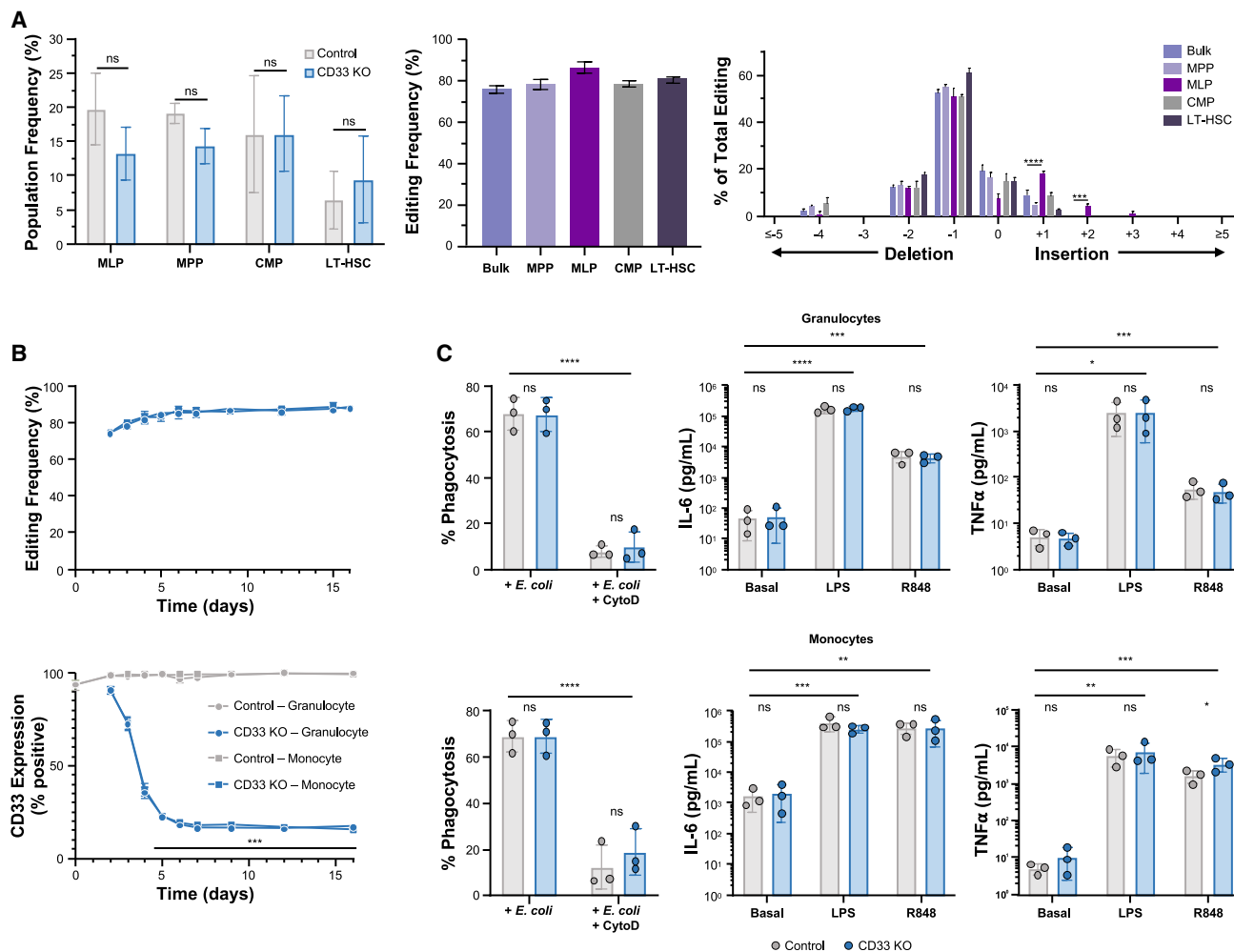


**Figure 2. CD33 KO does not impact HSPC populations or myeloid function**

(A) HSPC subpopulation frequency (percentage of total live cells) at 48 h post-electroporation in CD33-KO and control human CD34+ HSPCs. Mean  $\pm$  SD from three donors shown. Statistical analysis was performed using ANOVA with Šidák multiple comparisons test (left panel). Editing frequencies in the overall HSPC population (bulk) and each of the subpopulations were plotted as mean  $\pm$  SD from three donors (middle panel). Indel spectra from bulk and each subpopulation were plotted as mean  $\pm$  SD from three donors (right panel). MLP, multi-lymphoid progenitors; CMP, common myeloid progenitors; MPP, multipotent progenitors; LT-HSCs, long-term hematopoietic stem cells. (B) CD33-KO and control mobilized peripheral blood human CD34+ HSPCs from multiple donors were induced to differentiate down granulocytic or monocytic lineages. Editing frequency was assessed by ICE analysis. Flow cytometry was used to identify CD33<sup>+</sup> cells (indicated by percentages). Data are represented as mean  $\pm$  SD. (C) Myeloid function assessment in CD34+ HSPCs *in vitro* after myeloid differentiation. Phagocytic function of differentiated cells is shown as uptake of fluorescent *E. coli* bioparticles. Each dot represents one replicate; mean  $\pm$  SD shown by box and error bars. Statistical analysis was performed using two-way ANOVA comparing conditions with or without addition of cytochalasin: \*\*\*\* $p < 0.0001$ . Inflammatory cytokine secretion (IL-6, TNF $\alpha$ ) was evaluated. Each dot represents one replicate; mean  $\pm$  SD shown by box and error bars. Statistical analysis was performed using two-way ANOVA comparing unstimulated/basal condition versus lipopolysaccharide (LPS) stimulation, or basal condition versus R848 stimulation: \* $p < 0.05$ , \*\* $p < 0.01$ , \*\*\* $p < 0.001$ , \*\*\*\* $p < 0.0001$ . Two-way ANOVA with the Šidák multiple comparisons test was performed to compare CD33-KO versus control for each stimulation condition. IL-6, interleukin-6; LPS, lipopolysaccharide; TNF $\alpha$ , tumor necrosis factor alpha.

multilineage differentiation. For a CD33-KO graft to provide a beneficial therapeutic impact, LT-HSCs must be successfully gene edited while retaining the aforementioned attributes. There were no significant differences in the distribution of cell subpopulations between CD33-KO cells and control cells, including LT-HSCs, indicating that CD33 editing and consequent loss of CD33 protein does not skew the distribution of subpopulations (Figure 2A). The editing frequency and indel profile in the overall CD34+ HSPC population was

representative of each subpopulation, including LT-HSCs, and was like those observed in HL-60 cells, indicating that CD33 editing is not selective for specific subpopulations (Figure 2A). The exception was MLPs, which tended to have a higher number of insertions, even beyond +1 or +2 bp. This is somewhat expected due to expression of the enzyme terminal deoxynucleotidyl transferase in early lymphoid cells to facilitate V(D)J recombination, which favors insertions in NHEJ-based repair.<sup>24–26</sup>

### CD33 deletion did not affect myeloid cell differentiation and function

Since CD33 expression is mostly restricted to the myeloid compartment, we assessed the impact of editing on myeloid differentiation and function in CD33-KO HSPCs through *in vitro* differentiation to either monocytic or granulocytic lineages. CD33-KO and control cells were assayed for *CD33* gene editing throughout differentiation. In both monocytic and granulocytic lineages, >80% gene editing was achieved at 4 days post-electroporation (Figure 2B). In the CD33-KO arm, loss of CD33 surface protein was observed and stabilized at almost background level by day 5 after electroporation in both lineages, whereas there was no loss of CD33 expression in control cells (Figure 2B). Cells differentiated from CD33-KO HSPCs displayed the acquisition of standard myeloid markers (Figure S2) and cell function (phagocytosis, cytokine release) that were comparable with unedited control cells (Figure 2C), despite rapid and near-complete loss of CD33 surface expression.

### Trem-cel manufacturing at clinical scale is robust and reproducible

Based on the promising preclinical data, a scaled-up trem-cel manufacturing process was developed. The trem-cel product was manufactured reproducibly and reliably at two manufacturing sites. In 30 independently manufactured batches, we achieved clinically relevant doses ( $>3 \times 10^6$  viable CD34+ cells/kg) based on critical quality attributes (dose, viability, purity, editing efficiency, and residual T cells), despite variation in donor material, operator, and manufacturing sites (Figure 3A). CD34 enrichment was efficient, >90% of selected cells stained positive for CD34, <2% stained positive for the T cell marker CD3, and gene editing efficiency >70% was achieved (Figure 3A). We performed extended characterization on seven batches of trem-cel, including those used in pharmacology and toxicology assessments (described below). We also assessed the differentiation potential of trem-cel generated at clinical scale using colony-forming unit (CFU) assays and found no impact of editing on multilineage potential *in vitro* (Figure 3B). After monocyte differentiation, a substantial loss of CD33 surface expression was observed in trem-cel samples compared with controls, as was observed at research scale (Figure 3C).

### Trem-cel has no significant off-target effects

To ensure efficacy and safety of trem-cel, the gRNA must display high on-target editing efficiency for CD33 but minimal editing at off-target sites. We used an ensemble approach to enable rigorous assessment of unintended and off-target events (Figure 3D). Long-range PCR and PacBio long-read DNA sequencing revealed structural variation of <10% in CD33-KO cells with no foreseeable adverse impact as the primary mechanism of *CD33* disruption is preserved (Figure S3). G-banded karyotyping revealed no detectable gross chromosomal abnormalities across multiple batches of CD33-KO cells (both research and clinical scale), indicating that trem-cel displays preserved genomic stability (data not shown). We performed *in silico* and laboratory-based assays to nominate potential off-target sites. Sequence-based *in silico* prediction nominated

3,076 potential off-target sites. GUIDE-seq on four research-scale batches nominated a total of 29 potential off-target sites, with 10 sites shared with *in silico* prediction. The remaining 19 sites had moderate/poor homology (seven or more mismatch/gaps). In seven clinical-scale trem-cel batches, indel frequencies at nominated sites were assessed by hybrid capture sequencing. Sites sequenced with read depth of more than 500 in four out of seven batches were subject to further statistical testing following the previous study.<sup>27</sup> Across batches, no significant and reproducible off-target sites were observed (Figure 3D).

### *In vivo* pharmacology indicates maintenance of hematopoietic function in trem-cel

The mouse xenograft study assessed long-term engraftment and multilineage differentiation with trem-cel (Figure 4A). Comparison of the number of nucleated human blood cells showed no significant difference in chimerism or multilineage differentiation in the bone marrow (BM) in trem-cel-treated versus control mice (Figure 4B). As expected, there was loss of CD33 expression in the trem-cel samples, but no impact on myeloid cell frequency compared with control (Figure 4C). Similar trends were observed in peripheral blood (Figure S4) and spleen (Figure S5). This indicates that trem-cel manufactured at clinical scale persists long-term in hematopoietic tissue and supports effective multilineage repopulation and proper functioning of CD33-null HSPCs in mice.

Assessment of BM samples showed persistence of *CD33* editing at week 16 in all engrafted animals and maintenance of indel distribution pattern. The most common indels (1-bp and 2-bp deletions) persisted from trem-cel input material to each engrafted BM sample, indicating no selective advantage or disadvantage for a specific indel after engraftment of edited cells (Figure 4D).

CFU assays of mouse BM samples after long-term of engraftment of trem-cel showed no differences versus control samples in the numbers of multipotent hematopoietic progenitors giving rise to GEMM colonies, committed granulocyte-macrophage progenitor cells giving rise to GM/G/M colonies, and erythroid precursors that eventually differentiated into erythrocytes and formed BFU-E colonies (Figure 4E). Therefore, it can be concluded that lack of CD33 expression in trem-cel did not impact colony formation, indicating no impairment of early hematopoietic potential for differentiation. Quantification of genome editing events of single colonies derived from engrafted mouse BM showed that editing events were predominantly biallelic (Figure 4F), reflecting homozygous *CD33* KO and maintenance of biallelic editing. These observations align with those made following the same assessments in CD33-KO cells manufactured at research scale (data not shown).

### GLP toxicology assessment did not reveal significant adverse findings for trem-cel

In immunocompromised NSG mice receiving a single dose within 24 h of total body irradiation (Figure 5A), trem-cel was well-tolerated,

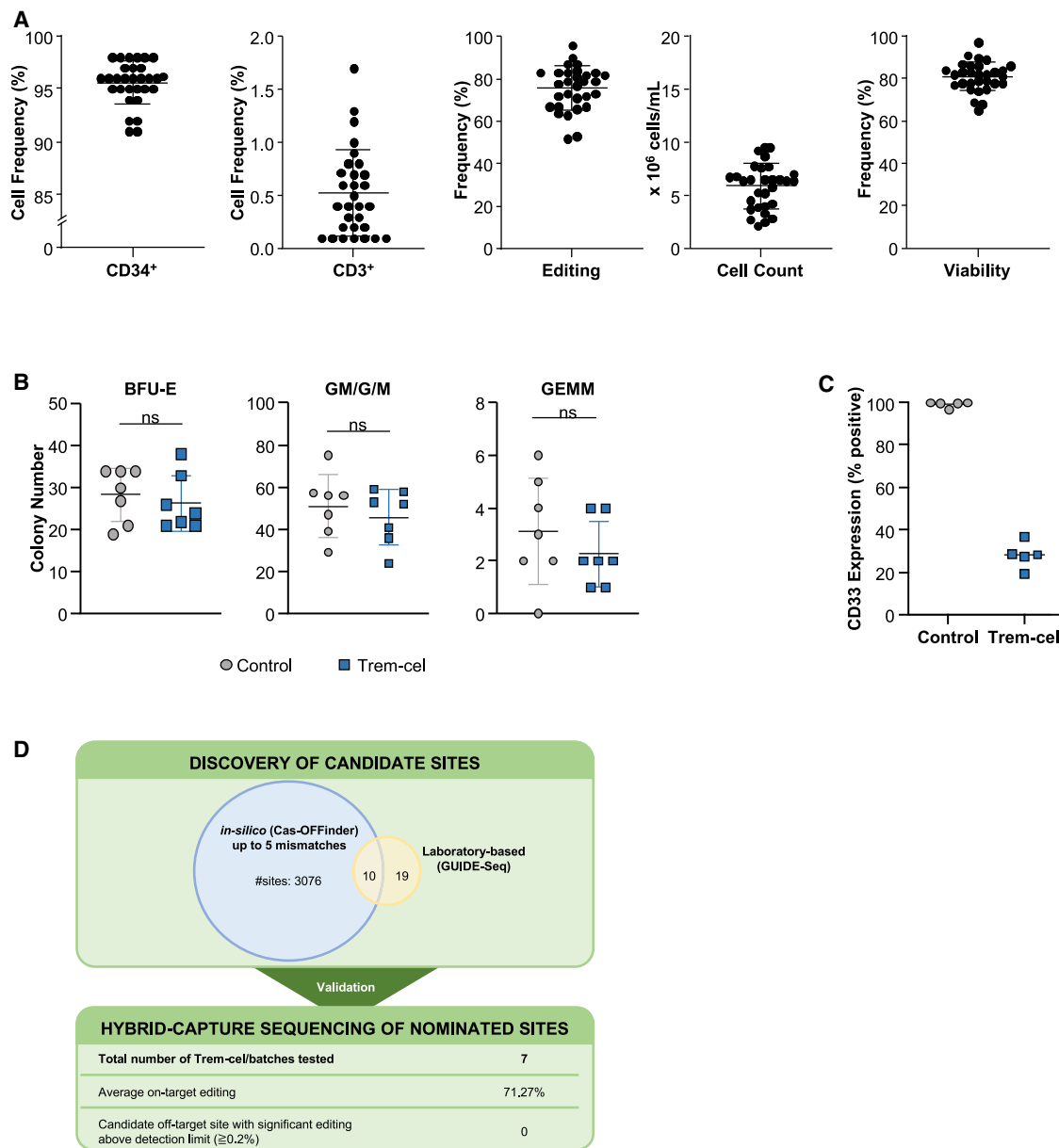


**Figure 3. Trem-cel manufacturing at clinical scale and characterization**

(A) Critical quality attributes of 30 batches of independently manufactured trem-cel products (dose, viability, purity, editing efficiency, and residual T cells) from two different sites. Each point represents a single batch and upper and lower horizontal lines indicated the standard error. (B) Quantification of BFU-E, CFU-GM/G/M, and CFU-GEMM colonies plated at 200 cells/plate for control and trem-cel-derived samples (seven batches each). The average number of colonies from two technical replicates across all batches is plotted. The horizontal lines represent mean of all batches. All p-values (Wilcoxon matched-pair signed rank test) for trem-cel versus control for all colony types were  $>0.05$ . (C) Loss of CD33 surface protein was assessed by flow cytometry in control and trem-cel-derived cells differentiated to monocytes (five batches each). Each symbol represents a single batch, the horizontal lines represent the mean  $\pm$  SD. (D) *In silico* and laboratory-based approaches used to nominate off-target editing events. Combined Fisher exact test (p value  $<0.05$ ) and  $>0.2\%$  indel frequency difference between edited and control samples were used to determine that no significant off-target sites were observed.

with no adverse effects attributed to trem-cel in any of the parameters assessed (hematology, clinical chemistry, and histopathology), and no abnormal clinical observations or mortality. Consistent with the previous *in vivo* studies, engraftment and multilineage differentiation in the BM (Figure 5B) and peripheral blood and spleen (Figure S6) were

unaffected in trem-cel samples in the bone marrow and CD33 editing was maintained over 20 weeks (Figure 5C). The dose tested in the toxicity study approaches the maximum feasible dose that can be administered intravenously in mice. Overall, the toxicology studies demonstrated a favorable safety profile for trem-cel.

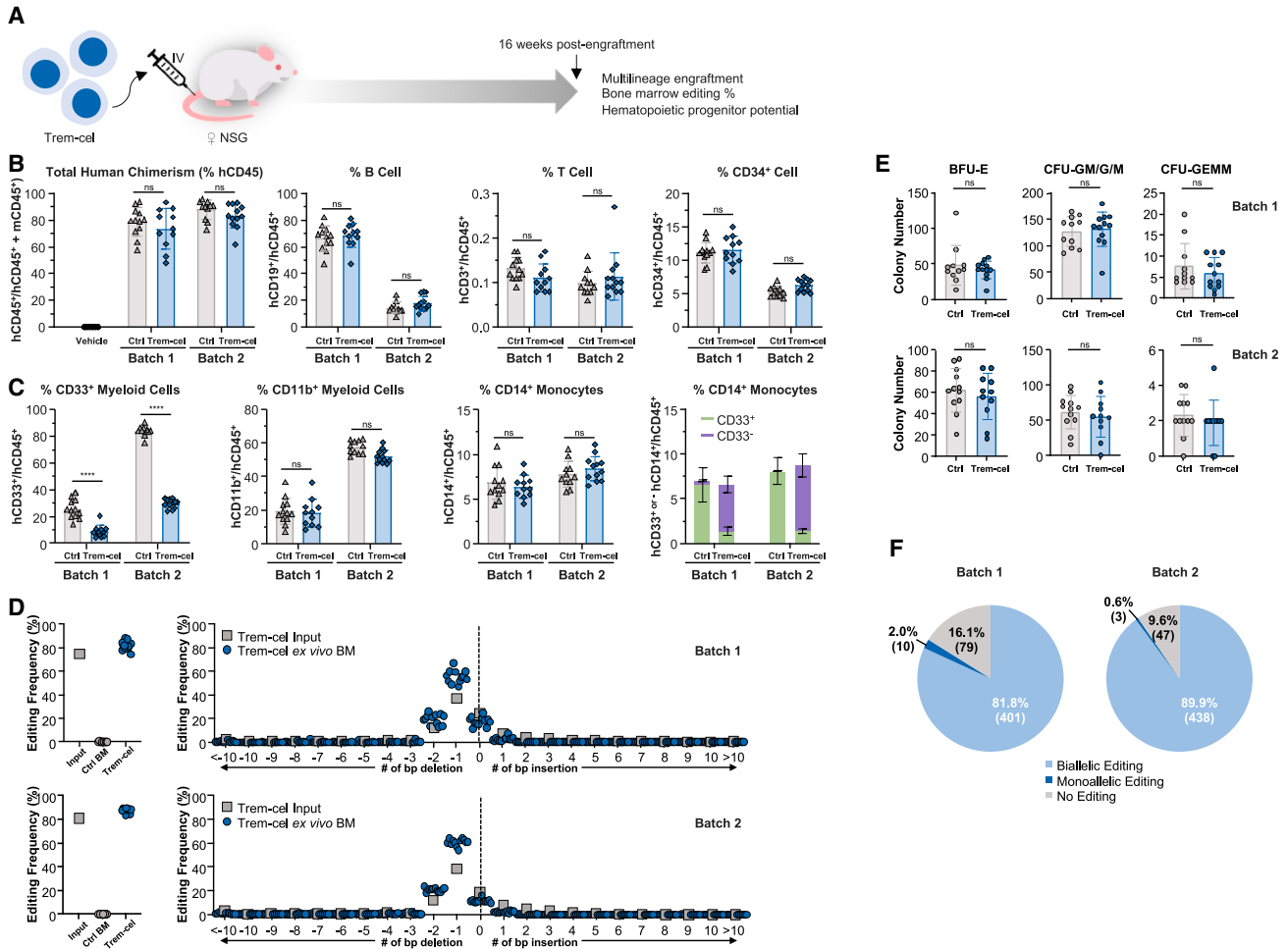


**Figure 4. In vivo pharmacology study**

(A) Experimental schema of xenotransplant study. (B) Chimerism and multilineage differentiation by flow cytometry. Levels of human CD45+ cell engraftment, and lymphoid (B cells: CD19+; T cells: CD3+) and (C) myeloid lineages in BM harvested from mice 16 weeks after engraftment of trem-cel (two independent batches). Each symbol represents one mouse; mean  $\pm$  SD are shown by box and error bars. \*\*\*\* $p < 0.0001$ ; ns, not significant ( $p > 0.05$ ) by unpaired t test ( $n = 12$  mice per condition). (D) (left panels) Total editing rates for all samples from two independent batches of trem-cel in BM from trem-cel engrafted and control mice. Cells used for engraftment (input) were included as an additional control. (right panels) Distribution of indel species in trem-cel-treated BM samples and trem-cel input cells. (E) Enumeration of BFU-E, CFU-GM/G/M, and CFU-GEMM colonies from engrafted samples plated at  $5 \times 10^4$  cells/well (two independent batches). Mean  $\pm$  SD shown by box and error bars; each dot represents one mouse. Top row represents trem-cel batch 1, bottom row represents trem-cel batch 2. (F) Single cell-derived CFU colonies were genotyped and categorized as biallelically edited, monoallelically edited, or unedited. The numbers indicated on the pie chart represent the percentage and number of colonies of each type.

### CD33-edited cells are resistant to CD33-directed therapies

As predicted, CD33-KO AML cell line HL-60 was resistant to GO cytotoxicity, whereas unmodified HL-60 cells were highly sensitive to GO (Figure 6A). The CD33-independent killing seen in the control line and at high GO doses, hypothesized to be an endocytosis mechanism, is consistent with previous observations seen at GO concentrations 100-fold or greater needed for blast saturation.<sup>28</sup>

In CD33-KO HSPCs generated at research scale, differentiated *in vitro*, and then exposed to GO, half maximal inhibitory concentration (IC<sub>50</sub>) values calculated from the dose-response curve were 29-fold higher (granulocytes) and 68-fold higher (monocytes) versus

control cells (Figure 6B), confirming that loss of CD33 protein protects myeloid cells from GO cytotoxicity.

An *in vitro* potency assay was conducted to assess the relationship between gene editing, CD33 surface protein loss, and resistance to GO. We assessed three independent batches, one generated at research scale and two at clinical scale. Gene editing frequency showed an inverse linear correlation with CD33 protein expression (Figure 6C). We observed an editing-dependent resistance to GO, where even a low editing frequency of 30% resulted in resistance compared with control cells. Higher editing frequency resulted in greater protection.

We next assessed if CD33-KO HSPCs or their progenies are resistant to GO cytotoxicity in a mouse model (Figure 6D). There was no impact on human chimerism or multilineage differentiation in the vehicle-treated control or CD33-KO animals (Figures 6E, 6F, and S7) as previously shown (Figures 4 and 5). Treatment with GO resulted in a significant reduction of CD33+ cells in control animals. Due to highly efficient editing in the donor human HSPCs (Figures 6G and S7), the CD33-KO group showed a near-complete loss of CD33+ cells irrespective of GO treatment (Figures 6E, 6F, and S7). GO treatment led to near-complete elimination of CD14+ monocytes in the BM of the control group, as CD14+ monocytes are almost all CD33+, whereas the CD33-KO group was resistant to GO-mediated toxicity displaying a 36- to 61-fold increase in the fraction of CD14+ monocytes versus controls (Figures 6E, 6F, and S7). The CD11b population also showed protection from GO treatment while the majority of CD11b+ myeloid cells in the control group were eradicated. These findings demonstrate that depletion of CD33 confers substantial resistance in myeloid cells against GO cytotoxicity *in vivo*.

## DISCUSSION

The preclinical, safety, and clinical scale-up studies reported here supported the clinical development of trem-cel, a gene edited allogeneic HSPC transplant for AML patients that has the potential of solving the on-target, off-tumor toxicity of CD33-directed therapies by increasing the therapeutic index. We have demonstrated a clinical-scale trem-cel manufacturing process that is robust, reproducible, and reliable. Preclinical studies showed proof-of-concept for CD33 ablation using gene editing. Editing was highly efficient, with near-complete loss of CD33 surface protein, but no impact on overall HSPC cell populations or their distribution, including the frequency of LT-HSCs, which ultimately give rise to long-term engraftment after transplantation.<sup>29</sup> Trem-cel cells lacked expression of CD33 but maintained normal myeloid differentiation and function. This correlates with previous findings that naturally occurring homozygous LOF mutations in *CD33* do not appear to have any detrimental effects on health.<sup>14,16</sup> Coupled with the observation that the *CD33* gene is tolerant of protein-truncating variation, this provides compelling evidence of the functional redundancy of this molecule in humans and supports the removal of CD33 expression as a therapeutic approach. Loss of the CD33 protein did not appear to significantly alter the normal composition of the cell subpopulations in the reconstituted hematopoietic compartment, and although a slight but not significant decrease in chimerism was observed in some batches, long-term *in vivo* engraftment was unperturbed, and editing was maintained.

Importantly, CD33-KO cells were resistant to the cytotoxicity induced by the CD33-targeted agent GO both *in vitro* and *in vivo*, which aligns with previous studies demonstrating that cells with reduced or no CD33 expression are resistant to CD33-targeted therapies.<sup>15,19,20,30</sup> We did observe a batch-specific decrease of overall hCD45+ chimerism in mice transplanted with CD33-KO HSPCs treated with GO that had a lower input editing efficiency (Figure 6F compared with Figures 6E and S7). This further indicates that higher editing frequency and subsequent CD33 protein loss results in better protection. Potency

assays demonstrated a positive correlation between *CD33* gene editing and resistance to GO cytotoxicity. The robustness of these data indicates that gene editing can serve as a surrogate measure of resistance to CD33-targeted killing (i.e., a measure of potency).

The preclinical safety studies demonstrated a favorable safety profile for trem-cel with no apparent differences in the safety parameters assessed compared with unedited control cells. There were no trem-cel-related adverse effects observed in the toxicity study at the highest dose tested ( $1 \times 10^6$  cells/animal), which is >10 times higher than the proposed minimum dose for the human clinical trials, thus representing a high safety margin. No significant off-target editing was identified for trem-cel, with no discernable differences in off-target frequencies in batches generated using different lots of gRNAs, manufacturing scales, and the indel profile confirmed that the editing event was consistent. The assessment of off-target editing utilizes a rigorous and clinically translatable safety framework in which to evaluate genotoxicity in CD34+ HSPC-based cell therapies for the treatment of relapsed/refractory AML.

These data supported the initiation of a first-in-human, multicenter, Phase 1/2a clinical trial of trem-cel in patients with AML in the United States and Canada (NCT04849910), with neutrophil engraftment being the primary endpoint with secondary endpoints including platelet recovery, incidence of graft-versus-host disease, incidence of graft failure, incidence of GO-related toxicities, relapse-free survival, and overall survival. Trem-cel is the first gene-edited HSPC transplant candidate therapeutic in development for the treatment of hematological malignancies. The trem-cel clinical trial will also allow the true biological dispensability of CD33 to be studied for the first time in a clinical setting.

In the context of AML treatment, trem-cel is anticipated to mitigate the hematological toxicity associated with anti-CD33 cellular therapies. The strategy of identifying dispensable gene editing targets through analysis of human genetic databases and modifying them in normal hematopoietic cells opens a therapeutic window. This approach provides an important therapeutic framework for enabling selective tumor targeting by many of the cancer immunotherapies currently in development, with the potential to improve patient survival.

## MATERIALS AND METHODS

### Gene editing of CD33

CRISPR-Cas9 was utilized to genetically ablate *CD33*. A panel of gRNAs were designed to specifically target and disrupt exon 3, common to all transcripts (Figure S1).<sup>19</sup> The lead gRNA was identified after evaluation of candidate gRNAs for editing efficiency, molecular characterization, impact on cell function, and off-target analysis as described above. To generate CD33-KO cells, the Cas9 protein and the gRNA were co-delivered into cells as a pre-complexed ribonucleoprotein (RNP) via electroporation. Control cells were generated by mock electroporation without the Cas9-RNP cargo.

The CD33-expressing human myeloid leukemia cell line HL-60 was obtained from ATCC (Manassas, VA, USA). HL-60 cells were

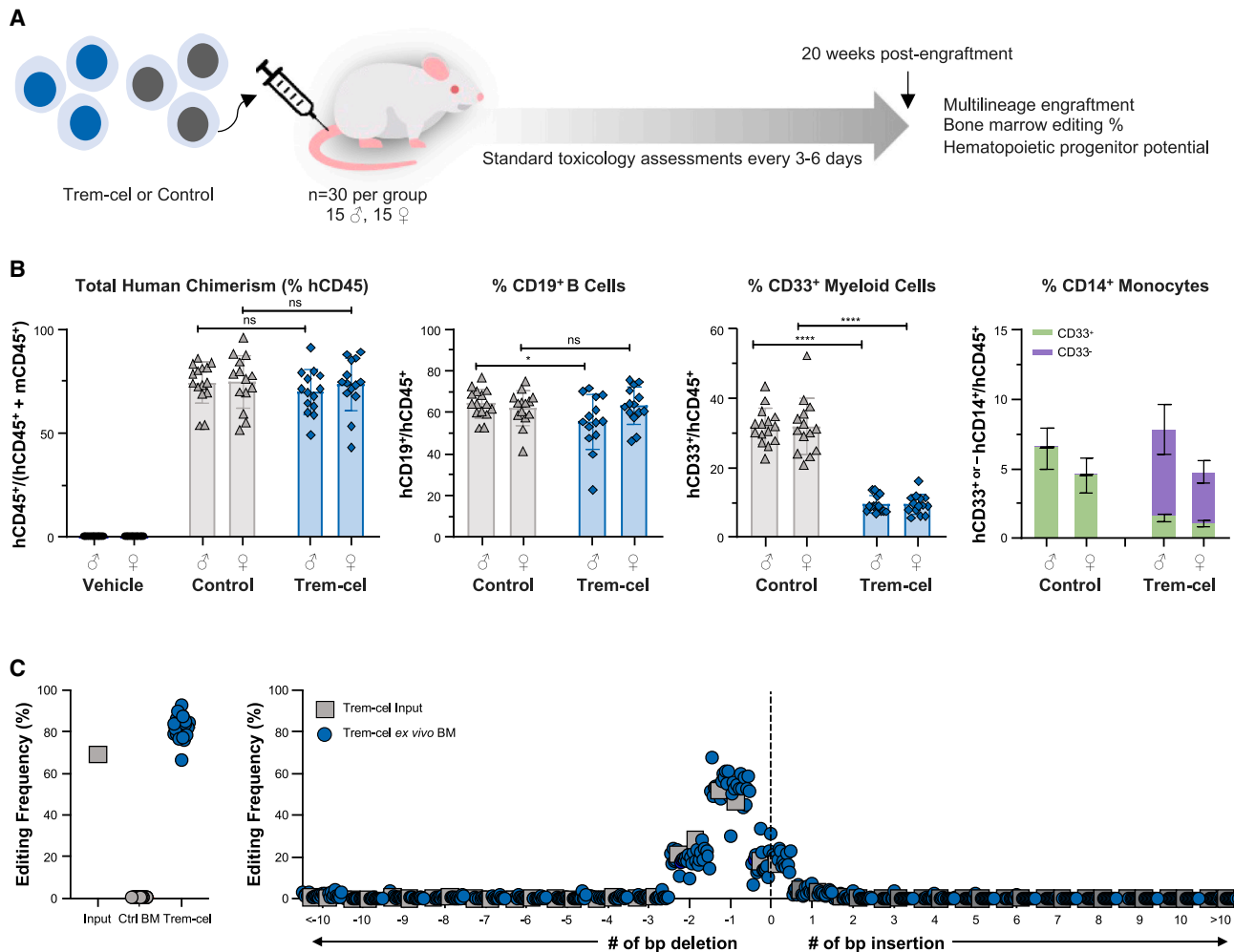


**Figure 5. Trem-cel *in vivo* toxicology study**

(A) Experimental schema of *in vivo* toxicology study. (B) Levels of human CD45<sup>+</sup> cell engraftment, and lymphoid (B cells: CD19<sup>+</sup>) and myeloid lineages in BM harvested from mice 20 weeks after engraftment of trem-cel. Data are shown separately for male and female mice. Each dot represents one mouse. Boxes and error bars show mean  $\pm$  SD. (C). (left panel) Total editing rates in input samples and BM from trem-cel-treated mice for all samples (right panel) Distribution of indel species in input samples and BM samples from trem-cel-treated mice.

electroporated on the Lonza Nucleofector system according to manufacturer's recommendations. To assess the molecular consequences of genetic ablation of *CD33*, CD33-KO and control HL-60 cells were cultured for 7 days and cells were collected every 24 h for analysis. The HL-60-derived CD33-KO cells described in Figure 6A were generated by electroporation of two unique CD33-targeting gRNAs.

In all instances, CD33 edited cells generated at research scale are referred to as CD33-KO cells, whereas the drug product generated at clinical scale is referred to as trem-cel (see below). To generate CD33-KO HSPCs at research scale, mobilized peripheral blood CD34<sup>+</sup> HSPCs from healthy human donors were obtained from Hemacare Donor Center (Northridge, CA, USA) and Stem Express (Folsom, CA, USA) and electroporated on the Lonza Nucleofector

system. The CD33-KO HSPCs described in Figures 6C and S7 were generated with an alternative CD33 exon 3-targeting gRNA.

#### Gene editing frequency

Genomic DNA was extracted for PCR amplification of the target genomic amplicon. Editing frequency and insertion or deletion (indel) event type was assessed by Sanger sequencing followed by inference of CRISPR edits (ICE).<sup>31</sup>

#### CD33 expression

CD33 RNA transcript expression was assessed by digital droplet PCR (ddPCR). Cells were counted on Nexcelom Cellometer K2 before RNA extraction via QIAGEN RNeasy Mini kit (Qiagen, Germantown, MD, USA). RNA was quantified via Qubit RNA BR



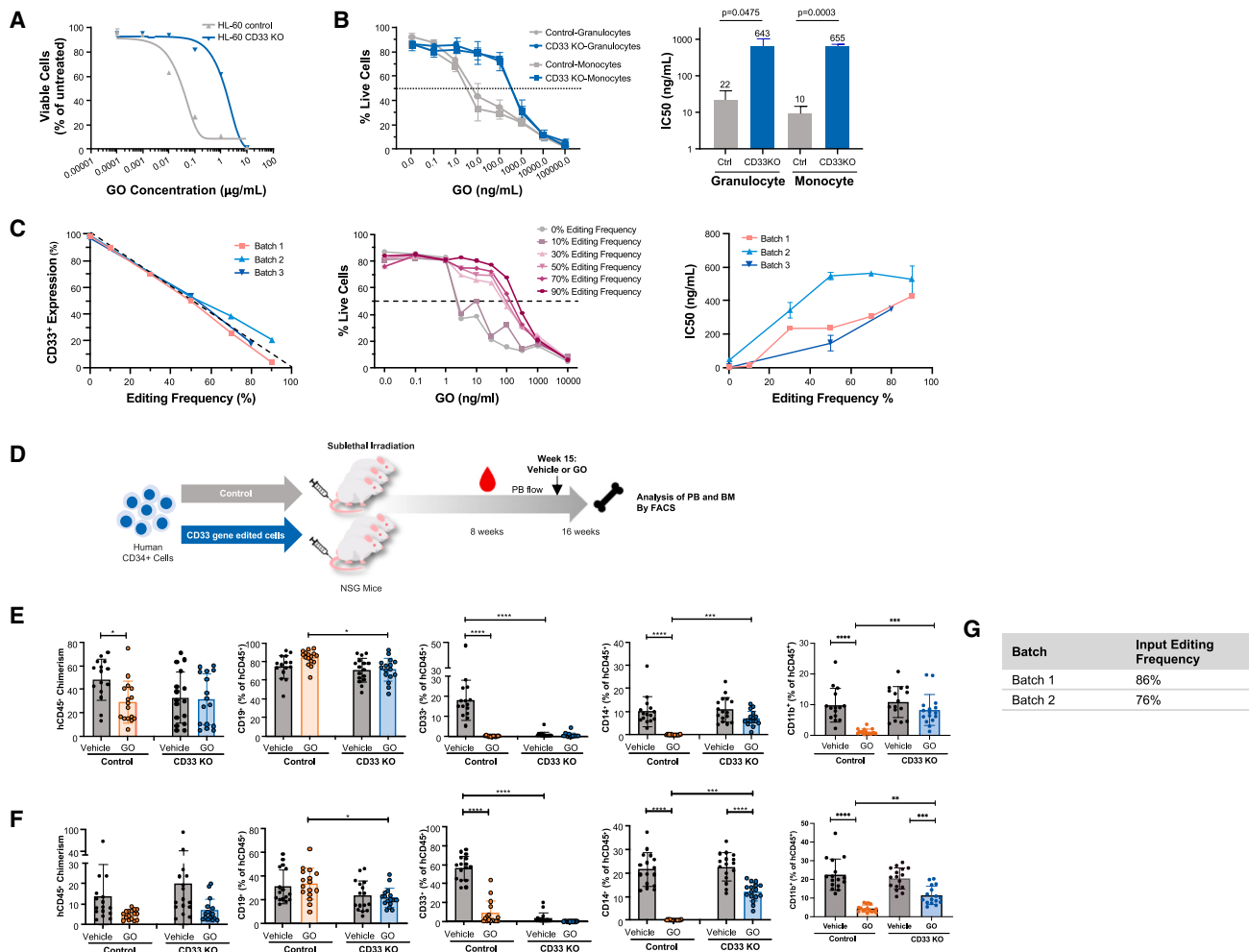


**Figure 6. CD33-KO cells are resistant to GO cytotoxicity**

(A) HL-60 CD33-KO and control cells were treated with increasing concentrations of GO for 72 h and the number of viable cells was determined by flow cytometry. (B) Following 7 days of myeloid differentiation to either granulocytes or monocytes, CD34<sup>+</sup> HSPC CD33-KO and control cells were exposed to increasing concentrations of GO for 72 h. Live cell percentages were determined by flow cytometry and dose-response curves were determined. IC<sub>50</sub> values were compared between CD33-KO and control cells using the unpaired Student's t test ( $p = 0.0475$  for granulocytic cultures and  $p = 0.0003$  for monocytic cultures). (C). Three separate batches of CD33-KO CD34<sup>+</sup> HSPCs were assessed (one research-scale, two clinical-scale trem-cel). CD33-KO cells were diluted with unedited cells to generate an editing titration curve from 10% to 90% editing frequency, with 90% being CD33-KO cells alone. Following 9 days of *in vitro* myeloid differentiation to monocytes, CD33 surface protein expression (flow cytometry) was correlated with CD33 editing frequency (ICE) (left panel). Cells were also exposed to increasing concentrations of GO for 72 h and live cell percentages were determined by flow cytometry, a representative sample (batch 1) is shown in the middle panel. IC<sub>50</sub> values were plotted for CD33-KO and control cells (right panel). (D) Experimental schema of the *in vivo* GO-challenge studies from two independent batches of CD33-KO cells. (E) Batch 1 and (F) Batch 2. Levels of human CD45<sup>+</sup> cell engraftment and lymphoid (CD19<sup>+</sup>) and myeloid lineages among total human leukocytes in the BM of CD33-KO engrafted and control animals were analyzed by flow cytometry. Each dot represents one mouse. Boxes and error bars show mean  $\pm$  SD. One-way ANOVA with Tukey's multiple comparisons test was used to compare between mice that received the same cells but different treatment (GO or vehicle), or to compare between mice that received the same treatment but different cells (CD33KO or control cells). (G). Input cell editing frequency determined by ICE.

(ThermoFisher, Waltham, MA, USA) before 100 ng of RNA extract was converted to cDNA via QuantiTech Reverse Transcript kit (Qiagen) and 0.5 ng of cDNA was utilized for ddPCR analysis. cDNA (0.5 ng), CD33 (6-FAM) (0.005 nmole probe/0.01 nmole primers) and ACTB (SUN) (0.005 nmole probe/0.01 nmole primers) primers (IDT, Coralville, IA, USA) were combined and utilized with ddPCR Supermix for Probes (Bio-Rad, Hercules, CA, USA) and analyzed

with Bio-Rad QX200 ddPCR System. The number of transcripts per sample was determined from positive droplets as analyzed with Bio-Rad QX Manager Software. The amount of CD33 transcript was normalized to both ACTB (a control gene), and a control sample as per the following equation: % of Mock = (CD33 sample/ACTB sample)/(CD33 of Mock/ACTB of Mock)  $\times$  100. The primer sequences are as follows: CD33 Primers (Forward: AACGTCACCTAT

GTTCCACAG; Probe:/6-FAM/CTCTTGTTT/ZEN/CCCTGAGCC ATCTCCTG/3IABKFQ;/ Reverse: CAGAGACAAAGAGCGAGCAG) and GUSB Primers (Forward: GCCCATT ATTCAGAGCGAGTA); Probe:/5SUN/TCATCCATG/ZEN/GTGAGCTGGCGG/3IABKFQ;/ Reverse: GTTTTTGATCCAGACCCAGATG).

CD33 protein expression was assessed by flow cytometry using a monoclonal anti-CD33 antibody. Cells were stained for 20 min in the dark at room temperature in fluorescence-activated cell sorting (FACS) staining buffer (Biolegend, San Diego, CA, USA). Live cells were identified by Live-Dead Near IR (ThermoFischer). CD33 surface protein expression was determined from the live population by anti-CD33 clone 67.6 (Biolegend, San Diego, CA) antibody via flow cytometry on either Cytek Aurora (Fremont, CA, USA) or Novocyte Quanteon (Santa Clara, CA, USA).

#### Analysis of HSPC subpopulations

At 48 h post-electroporation,  $2.4\text{--}6.5 \times 10^7$  CD33-KO HSPCs were sorted by FACS into the subpopulations of multi-lymphoid progenitors (MLPs), common myeloid progenitors (CMPs), multipotent progenitors (MPPs), and long-term hematopoietic stem cells (LT-HSCs) by gating on well-defined cell surface markers<sup>21,22,32</sup> using fluorescence minus one control cells. The frequency of each subpopulation was defined as the percentage of total live cells in each sample.

#### In vitro myeloid differentiation and functional assessment of HSPCs

At 48 h post-electroporation, CD33-KO and control CD34+ HSPCs were transferred into granulocytic or monocytic inducing media supplemented with cytokines (Stemcell Technologies, Cambridge, MA, USA) and cultured for 14 days. Assessment of differentiated lineages was performed at day 16 post-electroporation by flow cytometry using granulocytic and monocytic differentiation markers CD15 and CD14, respectively, and CD11b for pan-myeloid lineage. Functional assessment was performed by analysis of cytokine release and phagocytic capacity at day 16 post-electroporation.

Assessment of cytokine release was performed by stimulating differentiated cells with the Toll-like receptor (TLR) 4 agonist lipopolysaccharide (LPS) or the TLR7/8 agonist R848 for 24 h. Supernatant was then harvested and analyzed for interleukin (IL)-6 and tumor necrosis factor alpha (TNF $\alpha$ ; kits from Millipore Sigma, Darmstadt, Germany) using the Luminex FLEXMAP 3D platform (Luminex Corp., Austin, TX, USA). Phagocytic capacity was assessed using fluorescent pHrodo *E. coli* BioParticles (ThermoFisher Scientific, Waltham, MA, USA) and evaluated by flow cytometry. Cells were pre-treated with cytochalasin D, an inhibitor of actin-polymerization, which allows the assay to distinguish engulfment of particles from simple adhesion, the latter serving as the basal level of fluorescence for this assay.

#### Trem-cel manufacturing process development and scale-up

A scaled-up trem-cel manufacturing process was developed under Good Manufacturing Practice (GMP)-like conditions with GMP-

appropriate reagents for an anticipated clinical trial. The process was set up to achieve (1) sufficient cell viability and number of viable cells to enable HCT engraftment, (2) sufficient CD34+ cell purity without T cell contamination to reduce the risk of graft-versus-host disease, and (3) efficient gene editing to ensure protection from CD33-directed therapies.

Dual mobilized (G-CSF + plerixafor) hematopoietic stem cells from healthy donors were collected via apheresis from Hemacare Donor Center (Northridge, CA, USA) and Stem Express (Folsom, CA, USA). Dual mobilized (G-CSF + plerixafor) hematopoietic stem cells from healthy donors were collected via apheresis. The apheresis material was processed and washed to remove platelets and plasma. The washed cellular material was then enriched for CD34+ cells using positive selection with magnetic beads on a CliniMACS Prodigy system (Miltenyi Biotec, Gaithersburg, MD, USA). After selection, CD34+ hematopoietic cells were resuspended in MaxCyte electroporation buffer (MaxCyte Inc., Rockville, MD, USA), combined with a CD33-targeted ribonucleoprotein (RNP) comprising a single gRNA and Cas9 protein complexed immediately before use, and loaded into the MaxCyte GTx device for electroporation using the CL1.1 assembly. Post-electroporation, the cells were resuspended in SCGM media (Cellgenix) formulated with stem cell factor (SCF), Fms-related tyrosine kinase 3 ligand (FLT-3L), and thrombopoietin (TPO), cultured in a cell culture bag, and then the cells were centrifuged and washed to reduce cellular debris, cytokines, and other process-related residuals. These trem-cel cells were then resuspended in the final formulation buffer, transferred to an infusion bag, and cryopreserved in a controlled rate freezer and stored in liquid nitrogen. The entire manufacturing process is less than 5 days (Figure S8).

#### CFU assays

At 48 h post-electroporation, both trem-cel and control human CD34+ HSPCs were cryopreserved. Upon thaw, cells were plated in duplicate in MethoCult H4034 Optimum methylcellulose-based medium (Stemcell Technologies). After 14 days in culture, burst forming unit-erythroid (BFU-E), CFU-granulocyte/macrophage, granulocyte, and macrophage (CFU-GM/G/M) and CFU-mixed granulocyte, erythroid, macrophage, megakaryocyte (CFU-GEMM) colonies were imaged, analyzed, and quantified using STEMvision Human 14-day CFU Software (Stemcell Technologies). Colonies were scored and averaged from two technical replicates.

#### Off-target assessment

The presence of gross chromosomal abnormalities was assessed by G-banded karyotyping of metaphase spreads in several independent lots of CD33-knockout (KO) cells manufactured at research scale and trem-cel manufactured at clinical scale. Frozen edited and control cells were thawed and cultured in stem cell growth medium supplemented with cytokines (thrombopoietin, SCF, and FMS-like tyrosine kinase 3 ligand) and shipped at room temperature to Cell Line Genetics Inc. (Madison, WI, USA) for analysis using standard protocols and analysis.<sup>33</sup>

We performed *in silico* prediction of off-target sites using Genome Reference Consortium Human Build 38, in which sites containing a 5'-NRG-3' protospacer adjacent motif (PAM) sequence and (1) up to five mismatches with no indel; or (2) up to three mismatches and a one-base insertion or deletion (3) up to one and two mismatches in PAM region with up to three and two mismatches in guide regions, respectively, were predicted via a pipeline based on the Cas-OFFinder algorithm.<sup>34</sup>

For unbiased query of off-target sites, GUIDE-seq (for sequence homology-independent DNA double-stranded breaks)<sup>35</sup> was performed on research-scale CD33-KO cells. Nominated off-target sites from both *in silico* prediction and GUIDE-seq were assessed by a hybrid capture-based next-generation sequencing assay (Agilent, Santa Clara, CA, USA) using seven batches of clinical-scale trem-cel.

### ***In vivo* pharmacology**

*In vivo* pharmacology studies were performed in a xenotransplant mouse model to assess long-term engraftment, reconstitution of the hematopoietic compartment (multilineage differentiation), and persistence of editing. Two independent batches of clinical-scale trem-cel were assessed. Trem-cel was administered intravenously into immuno-compromised, sublethally irradiated NSG mice.

At week 16 post-engraftment, human hematopoietic lineage markers were assessed by flow cytometry analysis of blood, spleen, and BM samples. BM was also analyzed in CFU assays to determine human myeloid progenitor potential. Single colonies were picked 14 days after plating and subjected to Sanger sequencing to determine allelic editing.

To assess persistence of editing in engrafted cells, genomic DNA was extracted from BM samples and analyzed by targeting sequencing. PCR was used to amplify the template from a DNA sample using region of interest-specific primers with overhang Illumina adapters attached (Illumina, San Diego, CA, USA). Primers highly specific to the human genome were designed to avoid amplification of contaminating mouse genomic DNA that was present at ~50% level in the extracted genomic DNA. After using magnetic beads to purify the amplicon away from free primers and primer dimers, samples were indexed by limited-cycle PCR amplification using dual-indexed Illumina sequencing TruSeq adapters. Amplicon sequencing libraries were sequenced on the MiSeq System Sequencer (Illumina) using the 2 × 150 bp paired-end configuration.

### ***In vivo* toxicology**

In a 20-week Good Laboratory Practice (GLP)-compliant toxicity study, a single dose of trem-cel or control cells ( $1 \times 10^6$  cells/mouse) was administered into immunocompromised NSG mice (n = 30 per group; 15 male, 15 female) within 24 h of total body irradiation. All animals were observed for 20 weeks post-engraftment before being euthanized. Standard toxicology parameters were assessed including in-life observations every 3–6 days (e.g., clinical signs, food, and water consumption), hematology (12 parameters), organ weight (11 organs), clinical chemistry (19 parameters), and histopathology (43 pa-

rameters). The engraftment of human hematopoietic cells and persistence of editing was also assessed.

### **Resistance to anti-CD33 therapy cytotoxicity**

An *in vitro* cytotoxicity assay was performed on HL-60 CD33-KO and control cells to evaluate resistance to GO cytotoxicity. In this study, CD33-KO cells were generated using two gRNAs to delete CD33 exon 2. Dose-response curves were calculated after exposure to increasing concentrations of GO for 72 h. Live cell percentages were determined by flow cytometry analyses of apoptotic and necrotic cell staining.

*In vitro* cytotoxicity assays were also conducted using CD34<sup>+</sup> HSPCs from three donors. CD33-KO and control HSPCs underwent 7 days of myeloid differentiation to either granulocytes or monocytes, then were exposed to increasing concentrations of GO for 72 h. Live cell percentages were determined using annexin V and propidium iodide as markers for flow cytometry. Dose-response curves were plotted, and IC<sub>50</sub> values were calculated.

To determine the relationship between editing and cell surface protein loss, one batch of CD33-KO CD34<sup>+</sup> HSPCs generated at research scale and two batches of clinical-scale trem-cel were assessed. Edited cells were mixed with unedited cells at pre-determined ratios and subjected to the monocyte differentiation protocol described above. CD33 surface expression (determined by flow cytometry) was plotted against the expected calculated dose titration. Differentiated cells were also exposed to increasing concentrations of GO for 72 h as described above and IC<sub>50</sub> values calculated using a nonlinear fit model with absolute IC<sub>50</sub>.

*In vivo* cytotoxicity studies were also performed. Research-scale CD33-KO or control human HSPCs were engrafted in NSG mice as described for the *in vivo* pharmacology study. At ~15 weeks post-engraftment, mice were treated with GO or vehicle. Blood, spleen, and BM were collected for flow cytometry analysis at 16 weeks post-engraftment (8 days after GO/vehicle treatment) to determine resistance to GO cytotoxicity.

### **DATA AND CODE AVAILABILITY**

The data that support the findings of this study are available from the corresponding author upon reasonable request.

### **SUPPLEMENTAL INFORMATION**

Supplemental information can be found online at <https://doi.org/10.1016/j.omtm.2023.101135>.

### **ACKNOWLEDGMENTS**

We are thankful to our colleagues at Vor Biopharma for technical support and helpful discussions. Editorial assistance was provided by Helen Varley PhD, supported by Vor Biopharma. The graphical abstract and Figure S8 were created with [Biorender.com](https://biorender.com). All *in vivo* experiments complied with the relevant ethical regulations and regulatory standards for animal testing and research and were performed

under protocols approved by the Institutional Animal Care and Use Committee.

## AUTHOR CONTRIBUTIONS

J.R.L., M.I.L., H.G.G., S.M., and T.C. designed the research. A.H., S.W., M.B.J., J.E., G.A., J.X.F., J.L., K.S., Y.K., H.M., and J.S. performed research. All authors analyzed the data. J.R.L., M.I.L., H.G.G., and T.C. wrote the paper. All authors reviewed and approved the manuscript and agree to be accountable for all aspects of the work.

## DECLARATION OF INTERESTS

J.R.L., M.I.L., H.G.G., A.H., S.W., M.B.J., J.E., G.A., J.X.F., J.L., K.S., Y.K., H.M., J.S., J.H., and T.C. are salaried employees of Vor Biopharma Inc. and hold equity interests in the company. J.R.L., M.I.L., M.B.J., J.E., J.L., J.S., and T.C. are inventors on patent applications assigned to Vor Biopharma Inc. S.M. is a coinventor on patent applications related to this work, which were filed by Columbia University and are licensed to Vor Biopharma Inc. S.M. has equity ownership and is on the Scientific Advisory Board of Vor Biopharma Inc.

## REFERENCES

- De Kouchkovsky, I., and Abdul-Hay, M. (2016). Acute myeloid leukemia: a comprehensive review and 2016 update. *Blood Cancer J.* 6, e441. <https://doi.org/10.1038/bcj.2016.50>.
- N.A. Howlander N, M. Krapcho, D. Miller, A. Brest, M. Yu, J. Ruhl, Z. Tatalovich, A. Mariotto, D.R. Lewis, and H.S. Chen, et al., eds. (2020). *SEER Cancer Statistics Review, 1975-2017* (National Cancer Institute).
- Center for International Blood & Marrow Transplant Research (CIBMTR). US Summary Slides 2021. <https://cibmtr.org/CIBMTR/Resources/Summary-Slides-Reports>.
- O'Donnell, M.R., Tallman, M.S., Abboud, C.N., Altman, J.K., Appelbaum, F.R., Arber, D.A., Bhatt, V., Bixby, D., Blum, W., Coutre, S.E., et al. (2017). Acute Myeloid Leukemia, Version 3.2017, NCCN Clinical Practice Guidelines in Oncology. *J. Natl. Compr. Canc. Netw.* 15, 926–957. <https://doi.org/10.6004/jnccn.2017.0116>.
- Araki, D., Wood, B.L., Othus, M., Radich, J.P., Halpern, A.B., Zhou, Y., Mielcarek, M., Estey, E.H., Appelbaum, F.R., and Walter, R.B. (2016). Allogeneic Hematopoietic Cell Transplantation for Acute Myeloid Leukemia: Time to Move Toward a Minimal Residual Disease-Based Definition of Complete Remission? *J. Clin. Oncol.* 34, 329–336. <https://doi.org/10.1200/jco.2015.63.3826>.
- Levine, J.H., Simonds, E.F., Bendall, S.C., Davis, K.L., Amir, E.A.D., Tadmor, M.D., Litvin, O., Fienberg, H.G., Jager, A., Zunder, E.R., et al. (2015). Data-Driven Phenotypic Dissection of AML Reveals Progenitor-like Cells that Correlate with Prognosis. *Cell* 162, 184–197. <https://doi.org/10.1016/j.cell.2015.05.047>.
- Appelbaum, F.R., and Bernstein, I.D. (2017). Gemtuzumab ozogamicin for acute myeloid leukemia. *Blood* 130, 2373–2376. <https://doi.org/10.1182/blood-2017-09-797712>.
- Kenderian, S.S., Ruella, M., Shestova, O., Klichinsky, M., Aikawa, V., Morrissette, J.J.D., Scholler, J., Song, D., Porter, D.L., Carroll, M., et al. (2015). CD33-specific chimeric antigen receptor T cells exhibit potent preclinical activity against human acute myeloid leukemia. *Leukemia* 29, 1637–1647. <https://doi.org/10.1038/leu.2015.52>.
- Larson, R.A., Sievers, E.L., Stadtmauer, E.A., Löwenberg, B., Estey, E.H., Dombret, H., Theobald, M., Voliotis, D., Bennett, J.M., Richie, M., et al. (2005). Final report of the efficacy and safety of gemtuzumab ozogamicin (Mylotarg) in patients with CD33-positive acute myeloid leukemia in first recurrence. *Cancer* 104, 1442–1452. <https://doi.org/10.1002/cncr.21326>.
- Stein, E.M., Walter, R.B., Erba, H.P., Fathi, A.T., Advani, A.S., Lancet, J.E., Ravandi, F., Kovacsovics, T., DeAngelo, D.J., Bixby, D., et al. (2018). A phase 1 trial of vadastuximab talirine as monotherapy in patients with CD33-positive acute myeloid leukemia. *Blood* 131, 387–396. <https://doi.org/10.1182/blood-2017-06-789800>.
- Macaulay, M.S., Crocker, P.R., and Paulson, J.C. (2014). Siglec-mediated regulation of immune cell function in disease. *Nat. Rev. Immunol.* 14, 653–666. <https://doi.org/10.1038/nri3737>.
- Dhall, A. (2023). Unpublished Data; Analysis of the UK Biobank Database.
- Genome Aggregation Database (gnomAD) (2023). CD33 Molecule. [http://www.gnomad-sg.org/gene/ENSG00000105383?dataset=gnomad\\_r2\\_1](http://www.gnomad-sg.org/gene/ENSG00000105383?dataset=gnomad_r2_1).
- Sulem, P., Helgason, H., Oddson, A., Stefansson, H., Gudjonsson, S.A., Zink, F., Hjartarson, E., Sigurdsson, G.T., Jonasdottir, A., Jonasdottir, A., et al. (2015). Identification of a large set of rare complete human knockouts. *Nat. Genet.* 47, 448–452. <https://doi.org/10.1038/ng.3243>.
- Kim, M.Y., Yu, K.R., Kenderian, S.S., Ruella, M., Chen, S., Shin, T.H., Aljanahi, A.A., Schreeder, D., Klichinsky, M., Shestova, O., et al. (2018). Genetic Inactivation of CD33 in Hematopoietic Stem Cells to Enable CAR T Cell Immunotherapy for Acute Myeloid Leukemia. *Cell* 173, 1439–1453.e19. <https://doi.org/10.1016/j.cell.2018.05.013>.
- Genome Aggregation Database (gnomAD) (2023). Deletion (4 Bases): 19-51729103-CCCCG-C (GRCh37). [http://www.gnomad-sg.org/variant/19-51729103-CCCCG-C?dataset=gnomad\\_r2\\_1](http://www.gnomad-sg.org/variant/19-51729103-CCCCG-C?dataset=gnomad_r2_1).
- Brinkman-Van der Linden, E.C.M., Angata, T., Reynolds, S.A., Powell, L.D., Hedrick, S.M., and Varki, A. (2003). CD33/Siglec-3 binding specificity, expression pattern, and consequences of gene deletion in mice. *Mol. Cell Biol.* 23, 4199–4206. <https://doi.org/10.1128/MCB.23.12.4199-4206.2003>.
- Crocker, P.R., and Varki, A. (2001). Siglecs, sialic acids and innate immunity. *Trends Immunol.* 22, 337–342. [https://doi.org/10.1016/s1471-4906\(01\)01930-5](https://doi.org/10.1016/s1471-4906(01)01930-5).
- Borot, F., Wang, H., Ma, Y., Jafarov, T., Raza, A., Ali, A.M., and Mukherjee, S. (2019). Gene-edited stem cells enable CD33-directed immune therapy for myeloid malignancies. *Proc. Natl. Acad. Sci. USA* 116, 11978–11987. <https://doi.org/10.1073/pnas.1819992116>.
- Humbert, O., Laszlo, G.S., Sichel, S., Ironside, C., Haworth, K.G., Bates, O.M., Beddoe, M.E., Carrillo, R.R., Kiem, H.P., and Walter, R.B. (2019). Engineering resistance to CD33-targeted immunotherapy in normal hematopoiesis by CRISPR/Cas9-deletion of CD33 exon 2. *Leukemia* 33, 762–808. <https://doi.org/10.1038/s41375-018-0277-8>.
- Notta, F., Zandi, S., Takayama, N., Dobson, S., Gan, O.I., Wilson, G., Kaufmann, K.B., McLeod, J., Laurenti, E., Dunant, C.F., et al. (2016). Distinct routes of lineage development reshape the human blood hierarchy across ontogeny. *Science* 351, aab2116. <https://doi.org/10.1126/science.aab2116>.
- Wu, Y., Zeng, J., Roscoe, B.P., Liu, P., Yao, Q., Lazzarotto, C.R., Clement, K., Cole, M.A., Luk, K., Baricordi, C., et al. (2019). Highly efficient therapeutic gene editing of human hematopoietic stem cells. *Nat. Med.* 25, 776–783. <https://doi.org/10.1038/s41591-019-0401-y>.
- Shin, J.J., Schröder, M.S., Caiado, F., Wyman, S.K., Bray, N.L., Bordi, M., Dewitt, M.A., Vu, J.T., Kim, W.T., Hockemeyer, D., et al. (2020). Controlled Cycling and Quiescence Enables Efficient HDR in Engraftment-Enriched Adult Hematopoietic Stem and Progenitor Cells. *Cell Rep.* 32, 108093. <https://doi.org/10.1016/j.celrep.2020.108093>.
- Gore, S.D., Kastan, M.B., and Civin, C.I. (1991). Normal human bone marrow precursors that express terminal deoxynucleotidyl transferase include T-cell precursors and possible lymphoid stem cells. *Blood* 77, 1681–1690.
- Komori, T., Okada, A., Stewart, V., and Alt, F.W. (1993). Lack of N regions in antigen receptor variable region genes of TdT-deficient lymphocytes. *Science* 261, 1171–1175. <https://doi.org/10.1126/science.8356451>.
- Purugganan, M.M., Shah, S., Kearney, J.F., and Roth, D.B. (2001). Ku80 is required for addition of N nucleotides to V(D)J recombination junctions by terminal deoxynucleotidyl transferase. *Nucleic Acids Res.* 29, 1638–1646. <https://doi.org/10.1093/nar/29.7.1638>.
- Chaudhari, H.G., Penterman, J., Whitton, H.J., Spencer, S.J., Flanagan, N., Lei Zhang, M.C., Huang, E., Khedkar, A.S., Toomey, J.M., Shearer, C.A., et al. (2020). Evaluation

- of Homology-Independent CRISPR-Cas9 Off-Target Assessment Methods. *CRISPR J.* 3, 440–453. <https://doi.org/10.1089/crispr.2020.0053>.
28. Jedema, I., Barge, R.M.Y., van der Velden, V.H.J., Nijmeijer, B.A., van Dongen, J.J.M., Willemze, R., and Falkenburg, J.H.F. (2004). Internalization and cell cycle-dependent killing of leukemic cells by Gemtuzumab Ozogamicin: rationale for efficacy in CD33-negative malignancies with endocytic capacity. *Leukemia* 18, 316–325. <https://doi.org/10.1038/sj.leu.2403205>.
29. Notta, F., Doulatov, S., Laurenti, E., Poepl, A., Jurisica, I., and Dick, J.E. (2011). Isolation of single human hematopoietic stem cells capable of long-term multilineage engraftment. *Science* 333, 218–221. <https://doi.org/10.1126/science.1201219>.
30. Lamba, J.K., Chauhan, L., Shin, M., Loken, M.R., Pollard, J.A., Wang, Y.C., Ries, R.E., Aplenc, R., Hirsch, B.A., Raimondi, S.C., et al. (2017). CD33 Splicing Polymorphism Determines Gemtuzumab Ozogamicin Response in De Novo Acute Myeloid Leukemia: Report From Randomized Phase III Children's Oncology Group Trial AAML0531. *J. Clin. Oncol.* 35, 2674–2682. <https://doi.org/10.1200/JCO.2016.71.2513>.
31. Conant, D., Hsiao, T., Rossi, N., Oki, J., Maures, T., Waite, K., Yang, J., Joshi, S., Kelso, R., Holden, K., et al. (2022). Inference of CRISPR edits from Sanger trace data. *CRISPR J.* 5, 123–130. <https://doi.org/10.1089/crispr.2021.0113>.
32. Tomellini, E., Fares, I., Lehnertz, B., Chagraoui, J., Mayotte, N., MacRae, T., Bordeleau, M.É., Corneau, S., Bisailon, R., and Sauvageau, G. (2019). Integrin-alpha3 Is a Functional Marker of Ex Vivo Expanded Human Long-Term Hematopoietic Stem Cells. *Cell Rep.* 28, 1063–1073.e5. <https://doi.org/10.1016/j.celrep.2019.06.084>.
33. (2009). *Standards and Guidelines for Clinical Genetics Laboratories* (American College of Medical Genetics).
34. Bae, S., Park, J., and Kim, J.S. (2014). Cas-OFFinder: a fast and versatile algorithm that searches for potential off-target sites of Cas9 RNA-guided endonucleases. *Bioinformatics* 30, 1473–1475. <https://doi.org/10.1093/bioinformatics/btu048>.
35. Tsai, S.Q., Zheng, Z., Nguyen, N.T., Liebers, M., Topkar, V.V., Thapar, V., Wyvekens, N., Khayter, C., Iafrate, A.J., Le, L.P., et al. (2015). GUIDE-seq enables genome-wide profiling of off-target cleavage by CRISPR-Cas nucleases. *Nat. Biotechnol.* 33, 187–197. <https://doi.org/10.1038/nbt.3117>.